

Experiments and model predictions for fatigue crack propagation in riveted lap-joints with multiple site damage

R. Galatolo, R. Lazzeri

Department of Civil and Industrial Engineering, University of Pisa, Via Caruso, 56122 - Pisa, Italy

ABSTRACT

In this paper, the growth of long fatigue cracks up to failure in aircraft components is studied. A deterministic model is presented, able to simulate the growth of fatigue through cracks located at rivet holes in lap-joint panels. It also includes criteria to assess the link-up of collinear adjacent cracks in a MSD scenario. To validate the model, a fatigue test campaign was carried out on riveted lap-joint specimens in order to produce experimental crack growth and link-up data. Accurate measurements of naturally occurred surface cracks were performed automatically by the Image Analysis technique, thus allowing the tests to run 24 hours a day. The comparison between experimental tests and numerical simulations is good, thus confirming the model as a useful tool for the assessment of fatigue life of aircraft riveted joints.

Keywords: Fatigue crack growth, Numerical modelling, Crack interaction, Riveted joints, Image processing, 2024-T3 aluminium alloy.

NOMENCLATURE

a	crack length, see Tab. 1
$2a_{\text{eff}}$	effective crack length for the evaluation of secondary bending contribution to K_{tot} , see Tab. 1
C	parameter for crack propagation in the Paris law

CP_i	corrective factor to SIF due to the boundary conditions and rivet load
CP_{tot}	global corrective factor to SIF due to the boundary conditions and rivet load
CR_i	corrective factor to SIF due to the boundary conditions and uniform stress
CR_{tot}	global corrective factor to SIF due to the boundary conditions and uniform stress
d	diameter of the rivet
D	diameter of the squeezed rivet head
D/d	ratio between the diameter of the squeezed rivet head and the diameter of the rivet
E	Young's modulus
f	load frequency
K	contribution to Stress Intensity Factor due to membrane stress and pin loads
K_{bend}	contribution to Stress Intensity Factor due to secondary bending
K_c	fracture toughness
K_{tot}	Stress Intensity Factor
ΔK	Stress Intensity Factor range in the load cycling
m	parameter for crack propagation in the Paris law
N	number of cycles
p	uniform pressure on the hole due to the rivet, in a loaded joint
P	rivet load
$R = \sigma_{min} / \sigma_{max}$	stress ratio
t	specimen or panel thickness
w	specimen or panel width
w_{eff}	effective width for the evaluation of secondary bending contribution to K_{tot} , see Tab.1
$\gamma = \sigma_{bend} / \sigma_{\infty}$	bending ratio
ν	Poisson's ratio
σ_{bend}	stress due to secondary bending in lap-joints
σ_{bypass}	stress transferred by the rivets in a loaded joint

σ_{\max}	maximum value of the constant amplitude membrane stress
σ_{\min}	minimum value of the constant amplitude membrane stress
σ_{02}	yield stress
σ_{∞}	uniform membrane stress

INTRODUCTION

Fatigue design is a very important and critical phase during the development of aerospace components. At present, the Airworthiness requires the fulfilment of the damage tolerance criterion, but allows also the safe life criterion if the former is not applicable. Both criteria are based on the evaluation of crack propagation or crack nucleation, but only on deterministic bases, in spite of the deep stochastic nature of fatigue phenomena. So, high safety factors are required to prevent against uncertainties and unexpected events, generally resulting in heavy structures. Notwithstanding, high safety factors sometimes were not able to avoid failures because the real risk level is not known, as it happened in the Aloha accident¹ when a Multiple Site Damage (MSD) scenario was spread.

MSD is a serious question mainly connected with fatigue in ageing aircrafts^{2,3} but the presence of more than one crack and their interactions are problems that have to be faced also in other engineering fields.

Aerospace researchers are investigating the introduction of a new approach to fatigue design, based on probabilistic tools, which should control the risk level of components⁴, thus helping designers in making decisions in fleet strategy management⁵.

Some researchers have developed computer codes for the probabilistic life assessment of aerospace components with MSD, such as PROF⁶, SMART/LD⁷ and PISA (Probabilistic Investigation for Safe Aircrafts)⁸⁻¹¹.

In particular, one of the present authors developed the PISA code, which implements the Monte Carlo method to handle the statistical variables of the problem and allows the simulations of the fatigue life.

Briefly, the PISA code can manage deterministic inputs, such as joint geometries, and statistical inputs (e.g. statistical distributions of Equivalent Initial Flaw Size, EIFS, fracture toughness and coefficients of the fatigue crack growth rate law, fatigue loads). The EIFS is a fictitious initial crack dimension to be chosen in order to make the fatigue propagation life prediction from the EIFS to the final crack size at failure as similar to the actual experimental data as possible.

The code operates as follows: a random combination of initial flaws is applied at rivets holes of the joint, by drawing values from the EIFS distribution. Each flaw is then propagated according to the crack growth and link-up models, in order to calculate the number of cycles to joint failure. This procedure is repeated by randomly changing the combination of initial flaws, as well as the other statistical variables. Moreover, scheduled non destructive inspections and related probability of crack detection can also be treated by the code, introducing maintenance strategies and inspection intervals. In this way, after a huge number of numerical simulations, it is possible to calculate the probability of failure of the joint as a function of the inspection interval and the total operative life of the joint itself.

At present, USAF¹² requires for the aircraft structure of long-term military operations a probability of catastrophic failure at or below 10^{-7} per flight. In some cases¹³, even a lower probability of failure per flight is assumed, such as 10^{-8} . So, it is easily understandable that a high number of computer runs are necessary to evaluate the risk of failure by using the Monte Carlo method.

Of course, the probabilistic approach needs, as a background, an optimum knowledge and a deep understanding of fatigue phenomena, as well as reliable numerical models for fatigue damage prediction.

Fatigue phenomena can be divided into three main phases: crack nucleation, crack propagation and component failure. In some models, crack nucleation and crack propagation are often considered as an only propagation phase, starting from an 'adequate' EIFS¹⁴ at time zero.

Therefore, one among the most important points for the introduction of the probabilistic approach is the availability of reliable methods for the EIFS evaluation and for the crack growth simulation.

A previous experimental activity was carried out by the present authors to study the nucleation and the early propagation of short fatigue cracks emanating from rivet holes in lap-joint and butt-joint specimens.^{15,16} In that case, the crack growth mainly occurred in the hidden zone of the rivet holes, i.e. below the head of the countersunk rivets. As non-destructive inspection methods are not yet available with the requested accuracy, the crack size measurements were performed by opening the joint after a life percentage elapsed. Using this approach, each rivet hole of a specimen can give an experimental data point concerning the crack size at a particular number of cycles.

The aim of the present work is to complete the above theoretical and experimental activity by studying the subsequent long crack growth up to failure. Although this portion of the total life is smaller than that spent for crack nucleation and first propagation, it is not negligible. So it is important to evaluate it, in order to complete the whole life assessment of components.

In addition, MSD reduces the residual strength¹⁷ and causes a rapid increase in stress intensity factor. For these reasons, MSD and interactions among cracks should be taken into account in fatigue life evaluation.

In this paper, a model is presented to evaluate the growth of long fatigue cracks from rivet holes in lap-joint panels in a MSD scenario. The model also considers the interactions between collinear adjacent cracks and includes criteria to assess their link-up, thus enabling the prediction of the number of cycles to failure.

Such a model was implemented in the PISA code for a future simulation activity, not presented in this paper, to evaluate the probability of failure in riveted lap-joints.

To validate the crack growth model, an experimental activity was carried out on lap-joint specimens made of 2024-T3 aluminium alloy. The fatigue tests were performed using the Image Analysis (IA) technique to detect and measure the surface cracks out of the rivet heads. A computer code named FATIMA (FATigue crack measurement by the IMage Analysis technique)¹⁸ controls the testing machine and performs the measurements of the cracks. The measurements were performed automatically, thus allowing the tests to run 24 hours a day storing a high number of growth data points.

Finally, the crack growth predictions were compared with the experimental data giving very good results.

MATERIAL AND SPECIMENS

As mentioned above, in the present activity the attention was focused on the long crack growth, when cracks are longer than the rivet head and can be observed on the panel surface. The interactions between growing through cracks, before and after their link-up, were also of interest for this research. A specimen geometry similar to that adopted by Cavallini, Galatolo and Cattaneo¹⁶ was used: it consists of a 3-rows lap-joint panel with 15 countersunk rivets per row, where two columns of rivets near each boundary are more heavily squeezed to delay crack nucleation, as shown in Fig.1. In such a way, each panel has 22 possible crack nucleation sites, corresponding to the 11 rivets in the critical row shown in Fig. 1. As a matter of fact, the holes of this row are more heavily loaded, due to the countersunk holes and the secondary bending.¹⁹ Five lap-joint panels were tested, named BJ6, BJ7, BJ8, BJ9 and BJ10.

The sheet material is Al 2024-T3, thickness 2 mm ($E=72398$ MPa, $\nu=0.33$, $\sigma_{02}=331$ MPa, $K_c=45$ MPa m^{1/2}). Countersunk head solid rivets NAS 1097 AD6-7 in 2117-T4 aluminium alloy were used to joint the panels. No sealant was introduced in the joints.

The joints were realized with a rigorous quality control, as described in the work of Cavallini, Galatolo and Lazzeri¹⁵, so that they can be considered as belonging to the same family, thus avoiding a bias in the results. Particular care was put to rivet the specimens. A press was used to squeeze the heads by imposing a fixed displacement, thus ensuring the repeatability in order to obtain the prescribed $D/d=1.6$ ratio, i.e. the ratio between the diameter of the squeezed rivet head and the diameter of the rivet.

EXPERIMENTAL TECHNIQUE

All tests were carried out under constant amplitude loading with $\sigma_{\max}=120$ MPa, stress ratio $R=\sigma_{\min}/\sigma_{\max}=0.1$, and frequency $f=3$ Hz. They were performed on a 250 kN servo-hydraulic fatigue testing machine.

The IA technique was used to perform real-time measurements of the fatigue crack growth during the tests. Such technique consists of a periodic grabbing of images of the zone of a panel containing a growing crack. The images are digitised and converted into a matrix of pixels, containing the brightness information in a greyscale. The FATIMA code¹⁸ controls the testing machine and performs the measurements. Several additional algorithms were introduced in the code to solve the problems related to the recognition of the crack tip, when multiple cracks are present on the same rivet row interacting each other.

The FATIMA code controls the equipment shown in Fig.2: a Personal Computer (PC), an Analog-to-Digital (A/D) converter and a frame grabber plug-in cards, an optic-fibre illuminator, a black&white television camera fitted with high magnification lenses and a three-axes stage

equipped with step motors. At the beginning of the test, the television camera is manually moved, using the PC keyboard, to the critical sites from where a crack is expected to grow, i.e. both sides of each rivet head in the critical row. During the test running, FATIMA generates the control signal by the A/D converter and controls the testing machine in closed loop. When a measurement has to be performed, after a prescribed number of fatigue cycles, the load is kept constant at its maximum value; then a complete scan of the above sites is carried out and the real-time measurements are stored in the PC hard disk, together with the images for further checks after the end of the test.

The specimen preparation was limited to a rough polishing of the critical row by emery paper, just to remove the paint from the panel sheet in order to allow the recognition of the crack path. Due to the complete automation, it was possible to run the tests 24 hours a day. Each test was then terminated after reaching a prescribed total crack length, including possible link-ups.

The measurement accuracy depends on the magnification; the best results were obtained using magnification ranging from 5 to 10 $\mu\text{m}/\text{pixel}$. As the crack growth from each site could be higher than the field framed by the camera, the tracking of the crack tip was allowed. This aim was achieved by moving the camera and the illumination system by means of the same three-axes stage, thanks to suitable IA algorithms.¹⁸

It must be pointed out that the real-time measurement of fatigue cracks on a riveted lap-joint specimen represents a severe test for the FATIMA code, due to the secondary bending and to the round notches at the rivet holes; the former changes the light reflectivity of the specimen surface especially at large overall crack length after a link-up, while the latter makes difficult the recognition of the nucleation site because a hole is not a sharp notch. For these reasons, all the images grabbed during a test were also stored to be manually analysed after the end of the test. For example, Fig. 3 shows some images grabbed during the test on the BJ6 panel, relevant to the

adjacent cracks n. 18 and n. 19, after they emerged from the rivet heads until their link-up. In Fig. 4 a comparison between manual and automatic measurement of the same cracks is presented. It can be seen that most of the data are within the ± 0.5 mm lines, but sometimes the difference increases, when the cracks are near to link-up. As a matter of fact, plastic deformations are large in this situation, showing a bright path ahead of the crack tip (Fig. 3, N=87000). The IA algorithms thus easily mistook it for the crack tip. This is the case of crack n. 18 for which the last automatic measurement, occurred at cycle 87423, exceeds more than 1 mm the manual measurement shown in Fig. 4. However, the accuracy was enough to track the crack tip, during the test running, in order to automatically decrease the number of cycles between two measurements when the growth rate increases and to stop the test after reaching a prescribed total crack length. This feature is very important to reduce the testing time, because a complete scan of the rivet sites takes about two minutes, thus it is not convenient to carry out many measurements at the beginning of the test, especially for naturally occurring fatigue cracks. More accurate measurements were carried out after the end of the test by manually analysing the stored images.

THE CRACK GROWTH MODEL

The PISA code^{8,11} is a tool that simulates the fatigue behaviour of typical aerospace components, such as riveted lap joints, under a stochastic point of view. At present, the randomness is considered in nucleation (through the EIFS distribution), propagation (by means of the distribution of the parameters of the growth law), inspection actions and also final failure (through the fracture toughness K_c distribution). The Monte Carlo method is used in the code to handle different distributions for the stochastic variables in order to simulate a lot of different deterministic situations.

Of course, better deterministic models for the crack growth guarantee more reliable simulations and more accurate values for the probability of failure. At the same time, the chosen models have to be

as simple and versatile as possible to let an easy implementation inside the code with a minimum number of coefficients to handle as statistical inputs. For this reason, the present activity was focused on the validation of the deterministic models implemented in the code to compute the crack propagation, link-up and component failure.

The PISA code evaluates the crack growth by using the Paris law

$$\frac{da}{dN} = C \cdot \Delta K_{tot}^m \quad (1)$$

where the Stress Intensity Factor (SIF), K_{tot} , is calculated by using the composition and superposition of known simple solutions as a function of the boundary conditions²⁰. On this subject, Kuo, Yasgur and Levy²¹ collected lots of analytical expressions available in the literature, mainly obtained from the curve fitting of numerical results. The interactions among two or more cracks have been implemented in PISA through analytical expressions obtained by the authors from the best fitting of the curves for unequal length collinear cracks shown in the work of Rooke and Cartwright²².

Many researchers have investigated on the topic of crack interactions. Among them, Chang and Kotousov^{23,24} recently used the classical strip yield model and plasticity induced crack closure concept to develop and experimentally validate a new computational technique for the evaluation of interactions between through cracks. Wang, Modarres and Hoffman²⁵ used the Finite Element method to evaluate K at the tips of two collinear through cracks at adjacent holes and proposed a criterion to determine when crack growth is influenced by mutual interactions.

When all the corrective coefficient are evaluated, the contributions to the SIF due to the uniform membrane stress σ_∞ and that due to the pin loads P_i can be split as reported by Sampath and Broek²⁶ (Fig. 5):

$$K = \frac{1}{2} \cdot CR_{tot} \cdot (\sigma_{\infty} + \sigma_{bypass}) \cdot \sqrt{\pi \cdot a} + \frac{1}{2} \cdot CP_{tot} \cdot p \cdot \sqrt{\pi \cdot a} \quad (2)$$

where σ_{bypass} is the stress transferred by the rivets, $2a$ is the crack length and p is an uniform pressure on the hole, due to the rivet.

The panels under investigation were fastened to form a lap-joint, so that when they were loaded, not only uniform membrane stress was introduced in the panels, but also a certain amount of bending stress due to secondary bending. To take into account this effect, a bending ratio parameter $\gamma = \sigma_{bend} / \sigma_{\infty}$ ^{27,28} was introduced in the PISA code, where σ_{bend} is the maximum stress in the sheet due to the secondary bending. The effect of secondary bending can be taken into account as an additional addendum in K_{tot} evaluation:

$$K_{tot} = K + K_{bend} \quad (3)$$

where K_{bend} can be evaluated, according to the work of Sampath and Broek²⁶, as:

$$K_{bend} = \beta_{bend} \sigma_{bend} \sqrt{\pi a} \quad (4)$$

$$\beta_{bend} = 0.39 \cdot \left[1 + 0.16 \cdot \left(\frac{a_{eff}}{w_{eff}} \right)^2 \right] \quad (5)$$

The meaning of a_{eff} and w_{eff} is shown in Tab. 1.

This approach is simple and effective, although slightly conservative, as it has been demonstrated by M. Skorupa ~~M~~, A. Korbel, A. Skorupa ~~A~~ and T. Machniewicz²⁹.

The total corrective factors CR_{tot} and CP_{tot} are relevant to the uniform membrane stress and to the pin loads respectively. They are function of the geometric boundary conditions, such as holes, other

cracks, link-ups, finite width of the panel and countersink. The main corrective factors taken into account in the present work are summarized in Tab. 1. The total corrective factor for K contributions due to membrane stress and pin loads is then obtained by compounding the single contributions of the various factors to obtain:

$$CR_{tot} = CR_1 \cdot CR_2 \cdot \dots \cdot CR_n \quad (6)$$

$$CP_{tot} = CP_1 \cdot CP_2 \cdot \dots \cdot CP_n \quad (7)$$

The last case in Tab. 1 is relevant to the evaluation of the contribution due to secondary bending, K_{bend} .

Two collinear cracks are considered as linked according to the Swift criterion³⁰, i.e. when their plastic radii are tangential. The plastic zone size is evaluated through the Irwin's model.²⁰ Failure can be caused by reaching the yielding stress in the net section or the fracture toughness K_c .

Silva, Gonçalves, Oliveira and de Castro³¹, in the context of the EU funded SMAAC (Structural Maintenance for Ageing Aircraft) program, used a Finite Element approach to simulate the fatigue crack propagation in lap-joints made of 2024-T3 aluminium alloy. For failure prediction they proposed various methodologies, rather than the use of finite elements. Among them, the use of the net section plastic collapse procedure caused little differences between predicted and experimental results.

The present authors participated to SMAAC too^{11,16}. That research was the background for the follow-up activity herein shown. In the present work, net section is evaluated as the sum of the resistant ligaments between cracks, minus the plastic zones in front of the crack tips.

COMPARISON BETWEEN NUMERICAL PREDICTIONS AND EXPERIMENTAL RESULTS

The exact value of the bending ratio could be estimated by a Finite Element analysis of the joint, taking into account the geometry of the specimen, the stiffness of the rivets, the material of sheets and rivets, and the grabbing system of the testing machine. However, a reliable evaluation of the bending ratio $\gamma=0.85$ was alternatively computed by using an analytical model proposed by Schijve^{27,28}. So the growth predictions were performed using the minimum value for the bending ratio $\gamma=0$, the value $\gamma=0.85$ and the further value $\gamma=1$. In addition, a by-pass ratio of 0.66 was supposed, which is typical for 3-rows lap-joints with highly flexible fasteners.³² The constants C and m for the Paris law were assumed equal to $C=1.10885E-7$ mm/cycles and $m=2.9436$, following the experimental characterization of the same sheet material, as shown in the work of Lazzeri.³³ In that paper, the experimental results of 36 Center Cracked Tension specimens are shown. Specimen dimensions were $w=150$ mm and $t=2$ mm. A circular hole, diameter 4 mm, in the center of each specimen was artificially pre-cracked with two symmetric cracks of 1.5 mm in length. Fatigue crack growth tests were carried out at $R=0.1$ and $\sigma_{\max}=80$ MPa. The Paris law was assumed for crack growth simulation, while hole effect and finite width effect were taken into account for ΔK evaluation. So, each specimen gave one value for C and m coefficients. A lognormal distribution was then supposed for the 36 values of C, while a normal distribution was assumed for m.

The values of C and m used in the present paper correspond to the mean values of such distributions.

In this paper the crack growth simulations were started with an initial crack size equal to the first experimental measurement of the first crack, occurred at N_1 cycles. The growth simulation continued until N_2 cycles, N_2 being the number of cycles corresponding to the first detection of the second crack. The geometric configuration was then manually changed by introducing the second

initial crack, after which both the cracks were numerically propagated until the first detection of the third crack at N_3 , and so on. The geometric configuration was also changed when the growth simulation predicted a link-up of two adjacent cracks. In Tab. 2 the experimental crack scenario at the end of the tests is summarized. The total number of cracks, including small flaws detected after the joint tear down, was generally more than 20 for each specimen. The number of cracks appeared on the specimen surface, and thus measured by the IA technique, ranged from 6 to 11, giving 3-4 link-ups before the end of the test.

In Figs. 6 - 8 the comparison between experimental data and predictions made for $\gamma=0.85$ for three tests, panels named BJ6, BJ9 and BJ10, is shown. However, their behaviour are also representative for the other panels. In the figures, only few experimental data points are plotted, to let the graphs to be as clear as possible, but of course the experimental method allowed the recording of a large amount of experimental crack growth data.

It can be noted that the prediction for a single main crack growth is generally very good, as well as the first link-up between two cracks. The prediction is acceptable when more than two cracks are linked. However, in the latter configuration only few cycles are spent, so that the error made in the total number of cycles is very little.

The crack growth rate behaviour is shown in Fig. 9 for BJ6 specimen, together with the assumed Paris law. Looking at the first detected crack, crack 18, it can be seen that the central part of the propagation is very near to the Paris law. On the other hand, the growth rate is higher at the beginning and in the last part of the propagation. As far as the beginning is concerned, it must be pointed out that naturally occurring flaws start in the inner side of the lap-joint, at the hole of countersunk rivets (Fig. 10). So, during the hidden portion of the propagation, the crack front shape is strongly bent. When the crack appears on the surface, it grows faster than the far end of the crack front, until the front shape stabilizes, whereupon it shifts. As crack 18 approaches its opposite crack 19, going toward the link-up, the growth rate of both cracks is higher than predicted by Paris law. A

factor of two can be generally found only in the worst cases, i.e. at the very beginning of the surface propagation and just before a link-up.

Other cracks of specimen BJ6 behave in the same way, and similar results have been found for the other specimens.

To improve the crack growth predictions at the beginning, some changes could be introduced in the SIF calculation. As a matter of fact, a through-crack with a straight front was assumed in the present work for each measured surface crack, thus underestimating the SIF value. Denman, Baldwin, Taylor and Frey³⁴ carried out an experimental activity on similar riveted lap-joints, measuring the crack front shapes and describing the shape evolution with a fully populated second order equation with six coefficients. In the same work, the SIF was then calculated along the crack front. However, a FEM analysis for the specific geometry of the present lap-joint is not in the scopes of this work.

A tentative was done by the authors by assuming a straight through crack whose length was calculated as the average value between the surface measurement and the predicted length at the faying surface, according to the shape function proposed by Denman, Baldwin, Taylor and Frey³⁴. Initial crack growth rate data in Fig. 9 slightly moved toward the Paris law line, but the effects in terms of predicted life to the first link-up were quite limited.

As already said, many models have been presented in the literature concerning the propagation of interacting cracks up to link-up. In the approach proposed by Kotousov and Chang²⁴ the Paris law is modified by using the effective SIF range. In that paper, the comparison between measured and predicted crack growth, on sheet specimens with two collinear cracks, showed a difference of about 10% in life. Another solution is that proposed by Newman and Ruschau³⁵, by dividing the crack growth rate curve in multiple segments and using different Paris law coefficients for each segment. A similar approach was proposed by Sih³⁶ and Sih and Tang³⁷ by managing the transition between adjacent regions of the crack growth rate curve by using transitional functions. However, although such models can improve the crack growth predictions, they generally need a higher computational effort or use more coefficients. Since the main purpose of the present work is to evaluate simple

crack growth models to be used for probabilistic assessment, it is important to keep the number of statistical inputs as low as possible, in order to limit the computation time for the Monte Carlo simulations.

All the results are summarized in Tab. 3 and Tab. 4 for the first link-up and for the end of the test after the first crack detection respectively. Notwithstanding the above notes on growth rate, the results are good. In fact, the end of the test can be well predicted for the whole panels under the assumption $\gamma=0.85$, that is the value predicted by the Schijve's model. Indeed, predictions made without considering the secondary bending effect ($\gamma=0$) give higher values in terms of number of cycles to link-up and to failure than those experimentally obtained. This confirms the well known influence of secondary bending in lap-joint fatigue behaviour and the need to take it into account in numerical simulations.

The worst prediction for the first link-up assuming $\gamma=0.85$ is that concerning BJ7 (-35%). In this case it is not a matter of link-up between two cracks, but a crack going in the adjacent rivet hole. However, what is really different for this specimen with respect to the others is the crack scenario: the crack evolved to form a single long crack in a localized area, instead of resulting from the link-up of different cracks. In this case the secondary bending effect is quite different along the joint, so a single average value of γ cannot easily account for it. The errors presented in Tab. 3 for the other specimens ($\gamma=0.85$) range between -15% and +5.4%.

As far as the errors on panel failure predictions are concerned (Tab. 4, $\gamma=0.85$), the values range between -17.9% and +5.3%. Such results can be considered good, especially bearing in mind the complexity of the examined structural joint. More accurate results could be obtained with more sophisticated models, but the disadvantage of higher computational efforts is not compatible with the huge number of runs necessary for future probabilistic PISA code simulations.

CONCLUSIONS

In this paper, a model for the prediction of the fatigue crack growth in riveted lap joints with multiple site damage has been shown, taking the load path in the joint, the mutual interaction between collinear cracks and their link-up into account.

A test campaign was carried out on 2024-T3 riveted lap-joint specimens in order to validate the crack growth model. The joints were realized with a rigorous quality control, so that they may be considered as belonging to the same family, thus avoiding a bias in the results. An experimental test procedure, based on the IA algorithms implemented in the FATIMA code, allowed the automatic detection and measuring of surface cracks on the specimens as a function of the number of cycles. Crack growth predictions were carried out starting from the size of the first detected crack to the size of the cracks at the end of the test. A reliable value of the bending ratio $\gamma=0.85$ was estimated on the basis of the Schijve's results. The results are really satisfactory, as all the growth simulations are in good agreement with the experimental crack growth data.

In conclusion, the fatigue crack growth model herein presented demonstrated to give good results for a complex MSD scenario, even including the uncertainty on the bending ratio value.

The model was implemented in the PISA code for a future activity to assess the probability of failure of the same lap-joint panels.

ACKNOWLEDGEMENTS

The Authors gratefully thank the last year students Mario Emmi and Carmelo Introcaso for the technical support during testing activity.

Funding

This research was partially supported by the European Community in the context of the ADMIRE - Advanced Design concepts and Maintenance by Integrated Risk Evaluation for aerostructures – Project, (G4RD-CT-2000-00396).

DECLARATION OF CONFLICTING INTERESTS

The Authors declare that there is no conflict of interest.

REFERENCES

- 1 Hendricks W. (1991). The Aloha-airlines accident – A new era for aging aircraft, in Structural Integrity of Ageing Airplanes, S.N. Atluri, S.G. Sampath, P. Tong Eds., Springer, Berlin, 153-165.
- 2 Pitt S. and Jones R. (1997). Multiple-site and widespread fatigue damage in aging aircraft. *Eng. Fail. Anal.*, **4**, 237-257.
- 3 Schijve J. (1995). Multiple-site damage in aircraft fuselage structures. *Fatig. Fract. Eng. Mater. Struct.*, **18**, 329-344.
- 4 Tong Y. C. (2001). Literature review on aircraft structural risk and reliability analysis. DSTO-TR-1110 Doc., Aeronautical and Maritime Research Laboratory, Melbourne.
- 5 Inesta D., Miron E., Armigo J.I., Cabrejas J. and Boluda G. (2013). Fatigue and damage tolerance probabilistic approach for fleets of medium and large aircraft under military transport usage, In 27th Symposium of the International Committee on Aeronautical Fatigue, Jerusalem, Israel, 05-07 June 2013. Brot Editor, Jerusalem, Israel, pp. 1033-1052.
- 6 Berens A. P., Babish C. A. and Gallagher J. P. (2005). US Air Force risk analysis approach for aging aircraft. In 23rd Symposium of the International Committee on Aeronautical

- Fatigue, Hamburg, Germany, 08-10 June 2005. Dalle Donne Editor, Hamburg, Germany, 125-136.
- 7 Ocampo J., Millwater H., Singh G., Smith H., Abali F., Nuss M., Reyer M. and Shiao M. (2011). Development of a probabilistic linear damage methodology for small aircraft. *Journal of Aircraft*, **48**, 2090-2106.
 - 8 Cavallini G. and Lazzeri R. (2007). A probabilistic approach to fatigue risk assessment in aerospace components. *Eng. Fract. Mech.*, **74**, 2964–2970.
 - 9 Cavallini G. and Lazzeri R. (2012). A probabilistic approach to fatigue design of aerospace components by using the risk assessment evaluation, in ~~recent~~ Recent advances in aircraft technology, R.K. Agarwal Editor. InTech Publisher, Rijeka, Croatia, 29–48.
 - 10 Cavallini G., Lanciotti A. and Lazzeri L. (1997). A Probabilistic Approach to Aircraft Structures Risk Assessment. In 19th Symposium of the Int. Committee on Aeronautical Fatigue, Edinburgh, UK, 18-20 June 1997. Engineering Materials Advisory Services LTD Publishing, UK, 421-440.
 - 11 Lazzeri R. (2002). The PISA Code. *Aerotecnica Missili e Spazio*, **81**, 17-25.
 - 12 U.S. Department of Defense (2005). Aircraft Structural Integrity Program – MIL-STD-1530C.
 - 13 Lin K. Y. and Styuart A. V. (2007). Probabilistic Approach to Damage Tolerance Design of Aircraft Composite Structures. *Journal of Aircraft*, **44**, 1309-1317.
 - 14 Rudd J. L. and Gray T. D. (1978). Quantification of fastener-hole quality. *Journal of Aircraft*, **15**, 143-147.
 - 15 Cavallini G., Galatolo R. and Lazzeri R. (2001). Short crack growth in the lap joints: experimental and numerical results. In 21st Symposium of the International Committee on Aeronautical Fatigue, Toulouse, France, 27-29 June 2001. Cepadues Editions, Toulouse, France, 85-97.

- 16 Cavallini G., Galatolo R. and Cattaneo G. (1999). An experimental and numerical analysis of multi-site damaged butt-joints. In 20th Symposium of the International Committee on Aeronautical Fatigue, Bellevue, Washington, USA, 14-16 July 1999, Electronic Print Imaging Corporation (EPIC), Dayton, Ohio, USA, 177-201.
- 17 Galatolo R. and Nilsson K.F. (2001). An experimental and numerical analysis of residual strength of butt-joints panels with multiple site damage. *Eng. Fract. Mech.*, **68**, 1437-1461.
- 18 Galatolo R. (2002). Fatigue and Fracture Crack Measurement by the Image Analysis Technique. In: Proc. 8th Int. Fatigue Congress, *Fatigue 2002*. Stockholm, Sweden, 2-7 June 2002. Engineering Materials Advisory Services LTD Publishing, UK, 2611-2620.
- 19 Schijve J. (2009). Fatigue damage in aircraft structures, not wanted, but tolerated? *Int. J. Fatigue*, **31**, 998-1011.
- 20 Broek D. (1988). The practical use of fracture mechanics. Kluwer Academic Publishers.
- 21 Kuo A., Yasgur D. and Levy M. (1986). Assessment of damage tolerance requirements and analyses-task I report. ICAF Doc. 1583, AFVAL-TR-86-3003, Vol. II, AFVAL Wright-Patterson Air Force Base, Dayton, Ohio.
- 22 Rooke D.P. and Cartwright D.J. (1976). Compendium of Stress intensity factors. Her Majesty's Stationery Office, London.
- 23 Chang D. and Kotousov A. (2014). A fatigue crack growth model for interacting cracks in a plate of arbitrary thickness. *Fatig. Fract. Eng. Mater. Struct.*, **37**, 1254-1267.
- 24 Kotousov A. and Chang D. (2015). Theoretical and experimental study of fatigue growth of interacting cracks. *Int. J. Fatigue*, **70**, 130-136.
- 25 Wang X., Modarres M. and Hoffman P. (2009). Analysis of crack interactions at adjacent holes and onset of multi-site fatigue damage in aging airframes. *Int. J. Fracture*, **156**, 155-163.

- 26** Sampath S. and Broek D. (1991). Estimation of requirements of inspection intervals for panels susceptible to Multiple Site Damage. In *Structural integrity of aging airplanes*. Springer-Verlag, 339-389.
- 27** Schijve J. (1972). Some elementary calculations on secondary bending in simple lap joints, Report NLR TR 72036 U, Amsterdam (NL).
- 28** Schijve J., Campoli G. and Monaco A. (2009). Fatigue of structures and secondary bending in structural elements. *Int. J. Fatigue*, **31**, 1111-1123.
- 29** Skorupa M., Korbel A., Skorupa A. and Machniewicz T. (2015). Observations and analyses of secondary bending for riveted lap joints. *Int. J. Fatigue*, **72**, 1-10.
- 30** Swift T. (1993). Widespread fatigue damage monitoring – Issues and concerns. In *Proceedings of 5th International Conference on Structural Airworthiness of New and Aging Aircraft*, Hamburg 16-18 June, 1993, pp. 133-150. DGLR, Deutsche Gesellschaft für Luft- und Raumfahrt, Bonn
- 31** Silva L. F. M., Gonçalves J. P. M., Oliveira F. M. F. and de Castro P. M. S. T. (2000). Multiple-site damage in riveted lap-joints: experimental simulation and finite element prediction. *Int. J. Fatigue*, **22**, 319-338.
- 32** Soderberg J. (2012). A finite element method for calculating load distributions in bolted joint assemblies. LIU-IEI-TEK-A—12/01328-SE. Thesis work at Linköping University, Sweden.
- 33** Lazzeri R. (2005). Deterministic and Stochastic Models for fatigue crack growth rate characterization. XVIII AIDAA National Congress, Volterra (PI), Italy, 2005. INCOR-D.G.M.P. s.r.l., 1-16, (in italian).
- 34** Denman D. E., Baldwin J. D., Taylor B. M. and Frey M. J. (2001). Short crack evolution in countersink geometries. In *21st Symposium of the International Committee on Aeronautical Fatigue*, Toulouse, France, 27-29 June 2001. Cepadues Editions, Toulouse, France, 627-643.

- 35** Newman J. C. and Ruschau J. J. (2007). The stress-level effect on fatigue-crack growth under constant-amplitude loading. *Int. J. Fatigue*, **29**, 1608-1615.
- 36** Sih G. C. (2008). Anomalies concerned with interpreting fatigue data from two-parameter crack growth rate relation in fracture mechanics. *Theor. Appl. Fract. Mech.*, **50**, 142-156.
- 37** Sih G. C. and Tang K. K. (2014). Short crack data derived from the fatigue data of 2024-T3 Al with long cracks: Material, load and geometry effects locked-in by transitional functions. *Theor. Appl. Fract. Mech.*, **71**, 2-13.

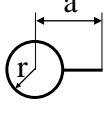
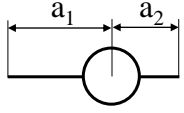

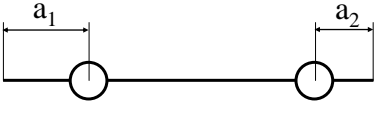
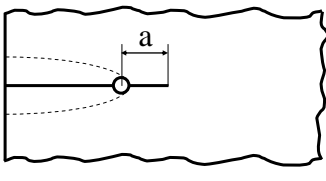
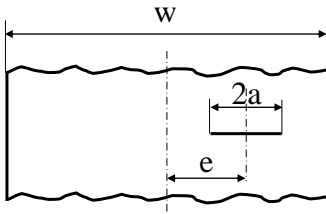
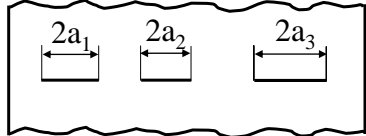
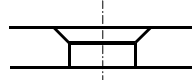
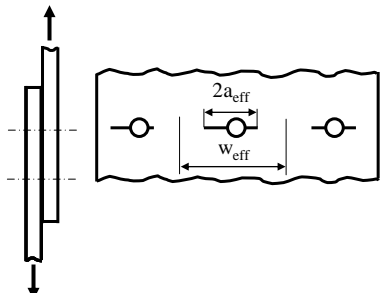
Captions for Tables

Tab.1 Main corrective factors to SIF calculation as a function of boundary conditions.

Tab. 2 Crack scenario at the end of the tests.

Tab. 3 Comparison between experimental test results and model prediction (first link-up).

Tab. 4 Comparison between experimental test results and model prediction (panel failure).

Crack at a hole ²¹	
Two cracks at a hole ²¹	
Link-up, with one crack ²¹	
Link-up, with two cracks ²¹	
Edge crack ²¹	
Panel finite width ²¹	
Interaction among cracks ²²	
Countersink ²¹	
Secondary bending ^{24,25}	

Tab.1 Main corrective factors to SIF calculation as a function of boundary conditions.

Test	N. of cracks at the end of the test	N. of through cracks at the end of the test	N. of link-ups at the end of the test	Cycles to first crack detection
BJ6	21	6	3	80925
BJ7	22	9	4	74000
BJ8	22	11	4	83300
BJ9	19	7	3	90000
BJ10	20	8	4	142300

Tab. 2 Crack scenario at the end of the tests.

Test	Cycles to first link-up (test data)	Cycles to first link-up after the first crack detection (test data)	γ	Cycles to first link-up (predictions)	Cycles to first link-up after the first crack detection (predictions)	First link-up after the first crack detection (error %)
	Cycles	Δ Cycles		Cycles	Δ Cycles	%
BJ6	87453	6528	0	92513	11588	77.5
			0.85	87813	6888	5.4
			1	87423	6498	-0.5
BJ7	88150	14150	0	92100	18100	27.9
			0.85	83200	9200	-35.0
			1	82200	8200	-42.0
BJ8	91400	8100	0	95600	12300	51.9
			0.85	91200	7900	-2.5
			1	91000	7700	-4.9
BJ9	100700	10700	0	105200	15200	42.1
			0.85	99100	9100	-15.0
			1	98100	8100	-24.3
BJ10	151700	9400	0	154800	12500	33.0
			0.85	151500	9200	-2.1
			1	151400	9100	-3.2

Tab. 3 Comparison between experimental test results and model prediction (first link-up).

Test	Cycles to the end of the test (test data)	Cycles to the end of the test after the first crack detection (test data)	γ	Cycles to the end of the test (predictions)	Cycles to the end of the test after the first crack detection (predictions)	Failure after the first crack detection (error %)
	Cycles	Δ Cycles		Cycles	Δ Cycles	%
BJ6	88323	7398	0	93913	12988	75.6
			0.85	88713	7788	5.3
			1	88113	7188	-2.8
BJ7	90910	16910	0	92900	18900	11.8
			0.85	90400	16400	-3.0
			1	83100	9100	-46.2
BJ8	93900	10600	0	97400	14100	33.0
			0.85	93000	9700	-8.5
			1	91400	8100	-23.6
BJ9	102298	12298	0	107200	17200	39.9
			0.85	100100	10100	-17.9
			1	98900	8900	-27.6
BJ10	152400	10100	0	155000	12700	25.7
			0.85	152100	9800	-3.0
			1	151500	9200	-8.9

Tab. 4 Comparison between experimental test results and model prediction (panel failure).

Captions for Figures

Fig. 1 Geometry of the lap-joint panel

Fig. 2 Sketch of the test equipment

Fig. 3 BJ6 panel – Images grabbed during the test

Fig. 4 Comparison between manual and automatic crack measurement

Fig. 5 Model for SIF calculation in lap joints due to σ_∞ and to pin loads

Fig. 6 Test results and model prediction (BJ6, $\gamma=0.85$)

Fig. 7 Test results and model prediction (BJ9, $\gamma=0.85$)

Fig. 8 Test results and model prediction (BJ10, $\gamma=0.85$)

Fig. 9 Experimental crack growth rate and Paris law prediction (BJ6, $\gamma=0.85$)

Fig. 10 Corner crack front evolution during crack propagation

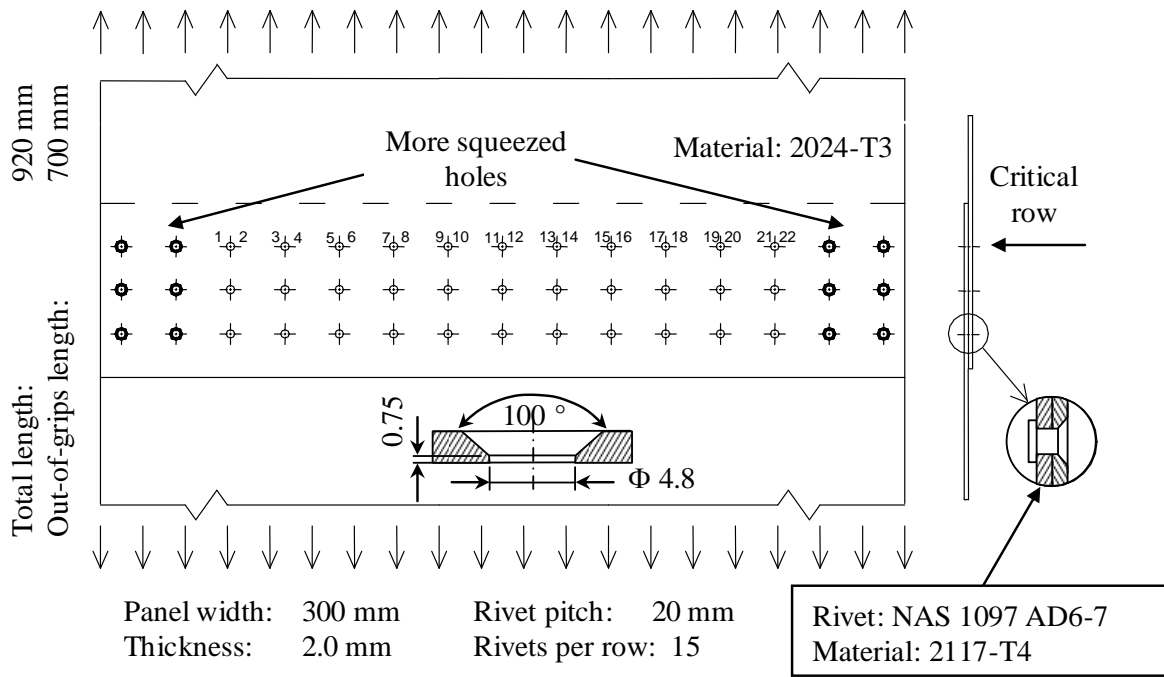


Fig. 1 Geometry of the lap-joint panel

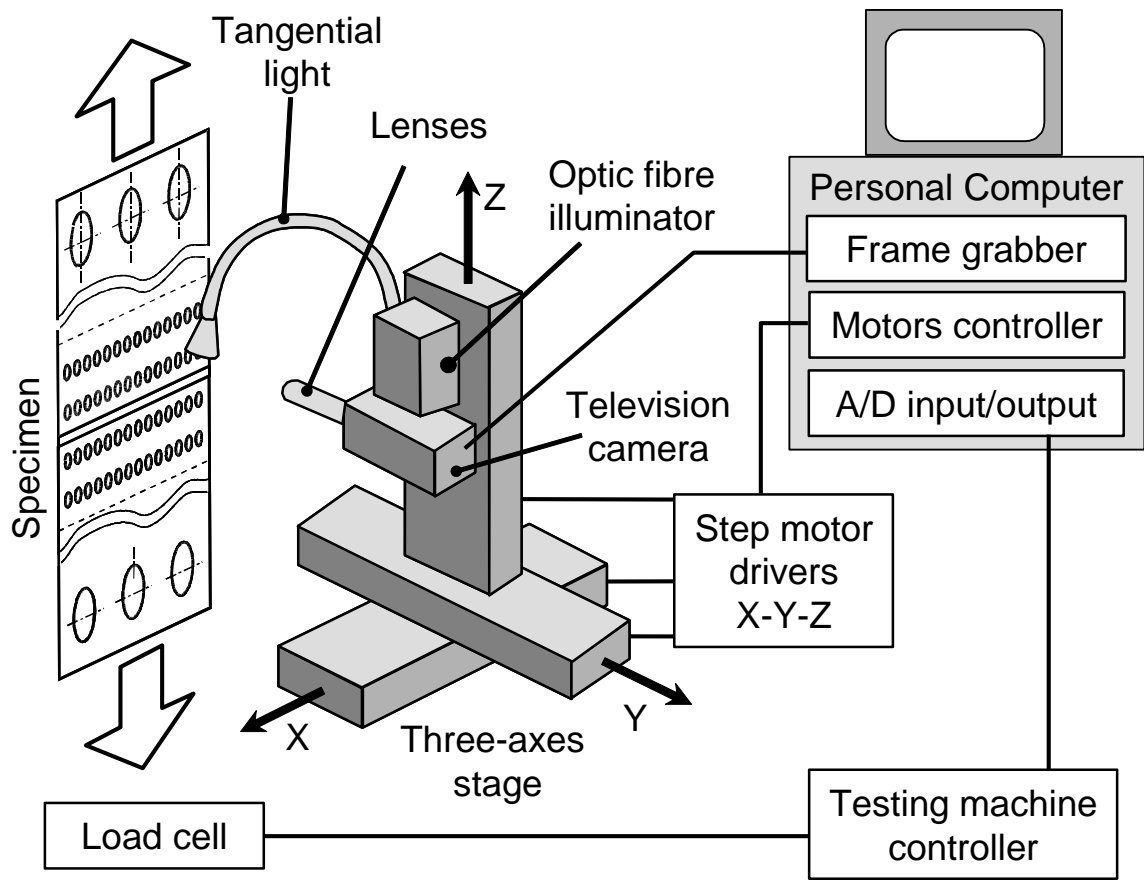


Fig. 2 Sketch of the test equipment

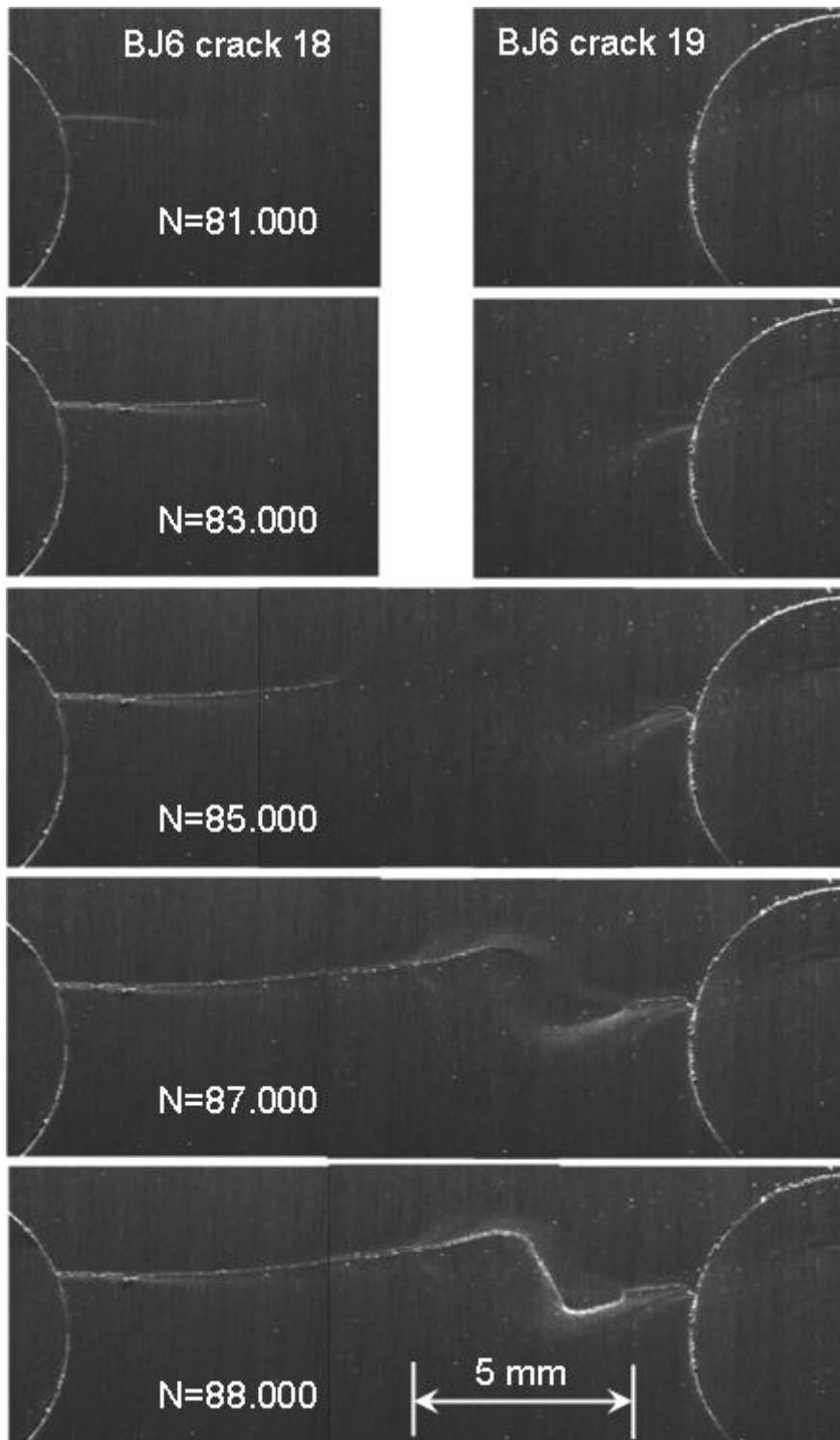


Fig. 3 BJ6 panel – Images grabbed during the test

BJ6 lap-joint specimen

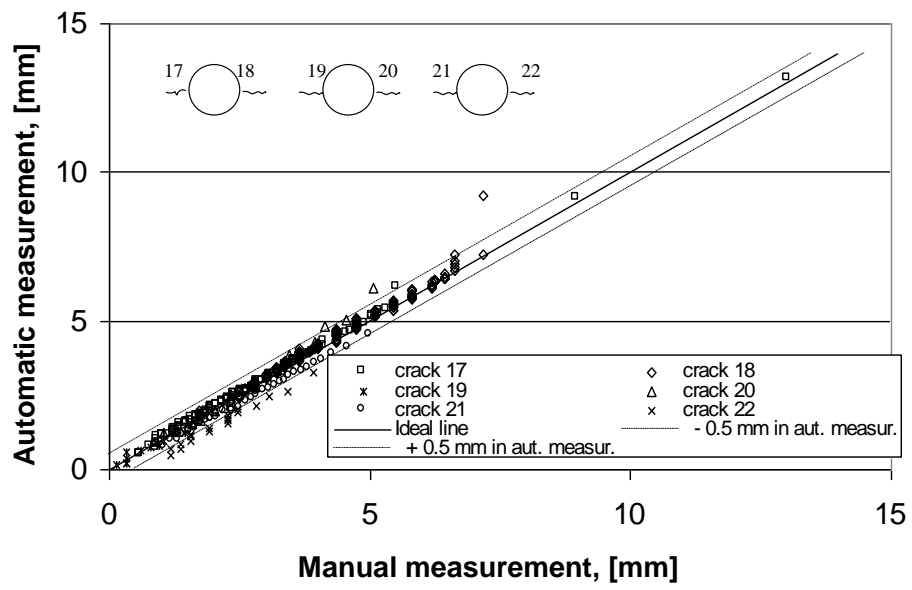
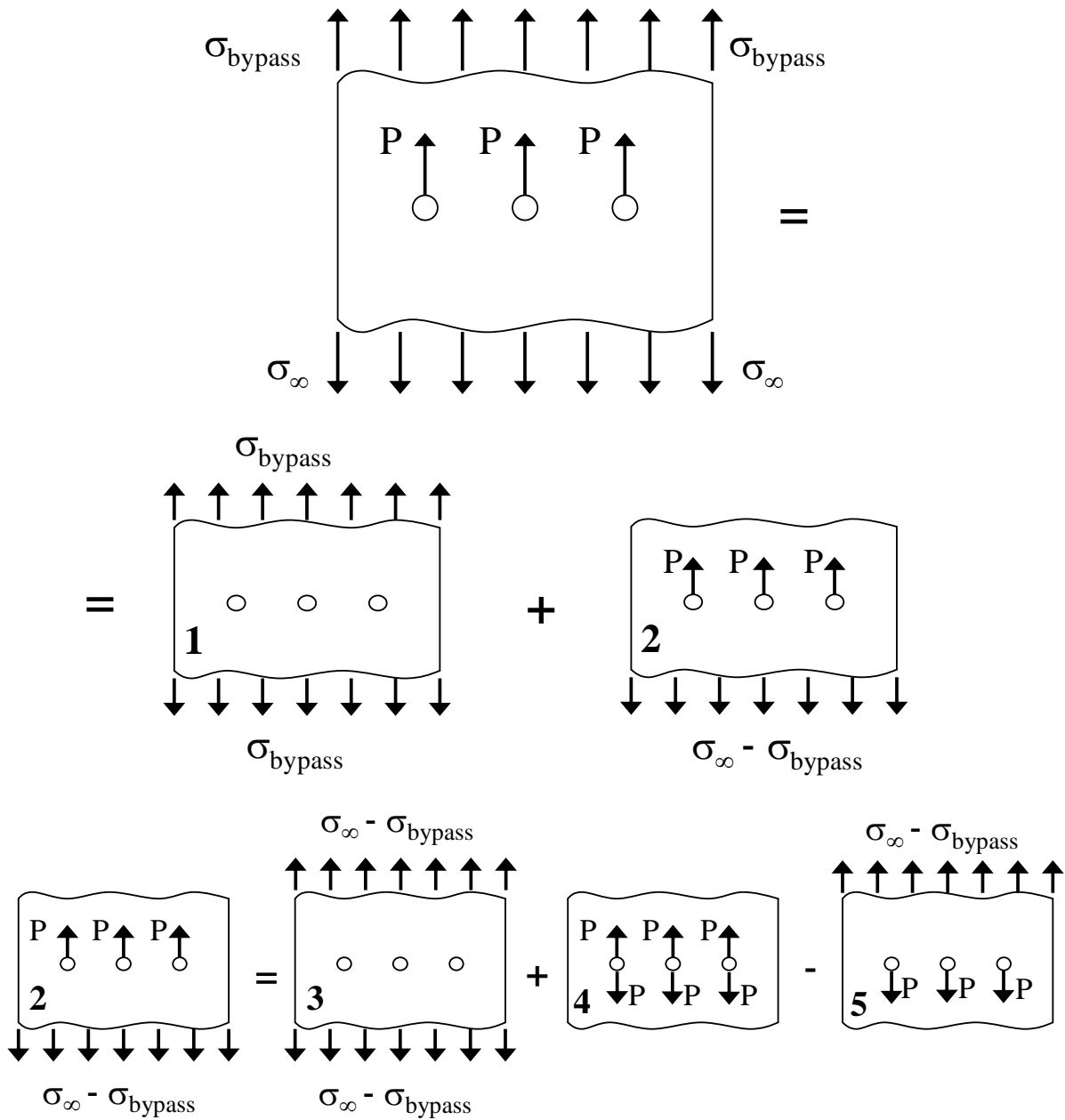


Fig. 4 Comparison between manual and automatic crack measurement



$$K = K_1 + K_2 = K_1 + \frac{1}{2} \cdot (K_3 + K_4)$$

$$K = CR_{tot} \cdot \left(\frac{\sigma_\infty + \sigma_{bypass}}{2} \right) \cdot \sqrt{\pi a} + \frac{1}{2} \cdot CP_{tot} \cdot p \cdot \sqrt{\pi a}$$

Fig. 5 Model for SIF calculation in lap joints due to σ_∞ and to pin loads

BJ6 - Comparison between experimental results and PISA simulation ($\gamma = \sigma_{\text{bend}} / \sigma_{\text{membr}} = 0,85$)

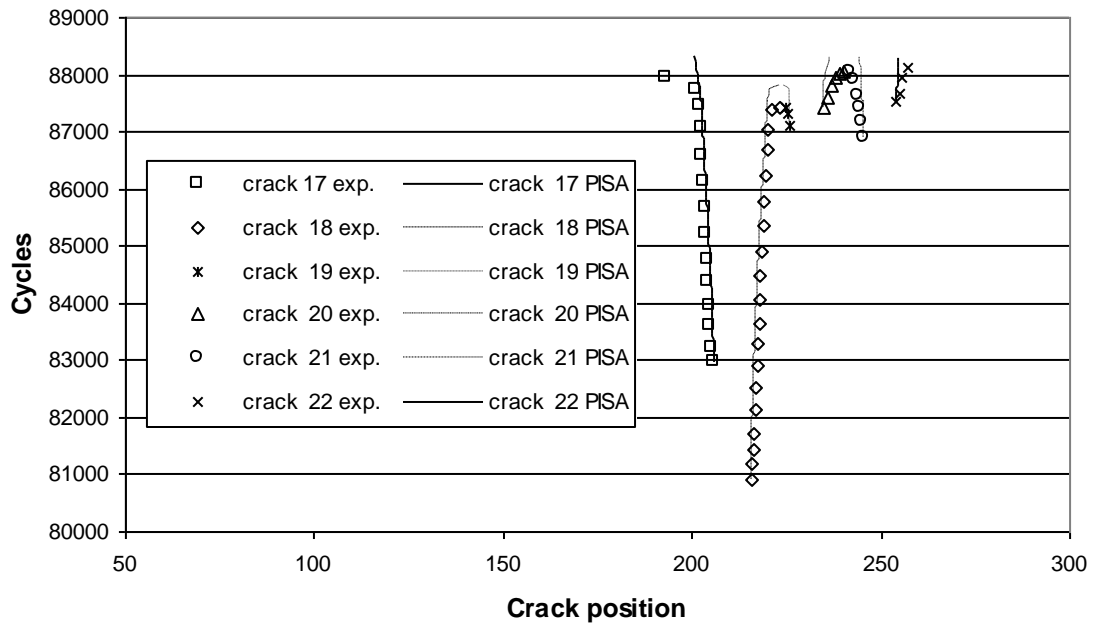


Fig. 6 Test results and model prediction (BJ6, $\gamma=0.85$)

BJ9 - Comparison between experimental results and PISA simulation ($\gamma = \sigma_{\text{bend}} / \sigma_{\text{membr}} = 0.85$)

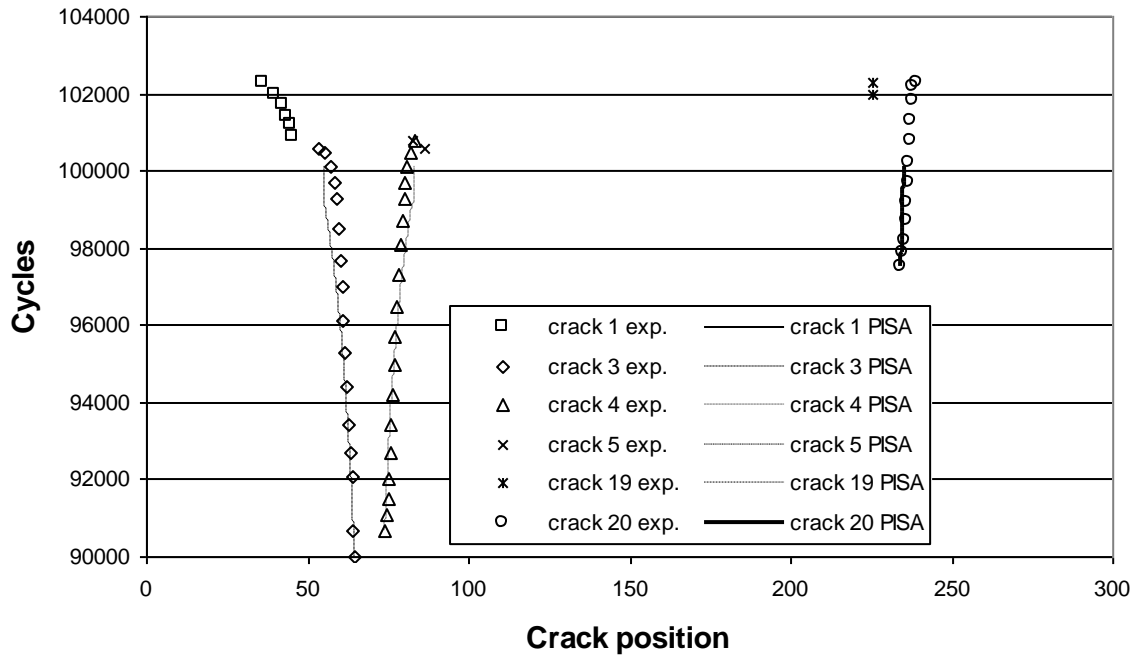


Fig. 7 Test results and model prediction (BJ9, $\gamma=0.85$)

BJ10 - Comparison between experimental results and PISA simulation ($\gamma = \sigma_{\text{bend}} / \sigma_{\text{membr}} = 0.85$)

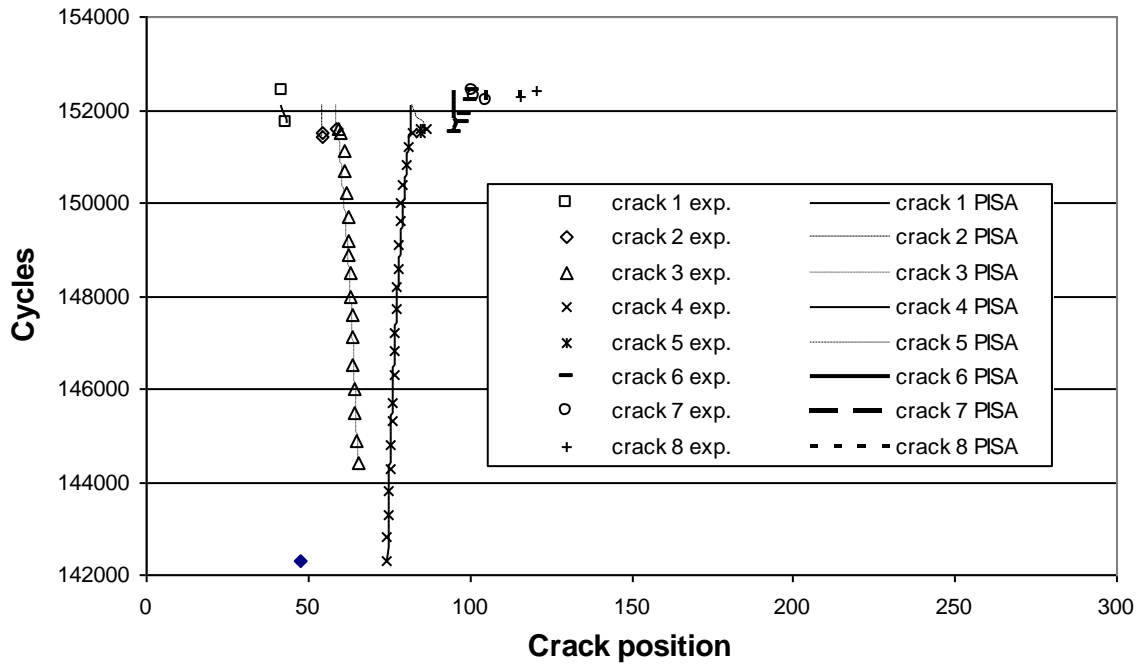


Fig. 8 Test results and model prediction (BJ10, $\gamma=0.85$)

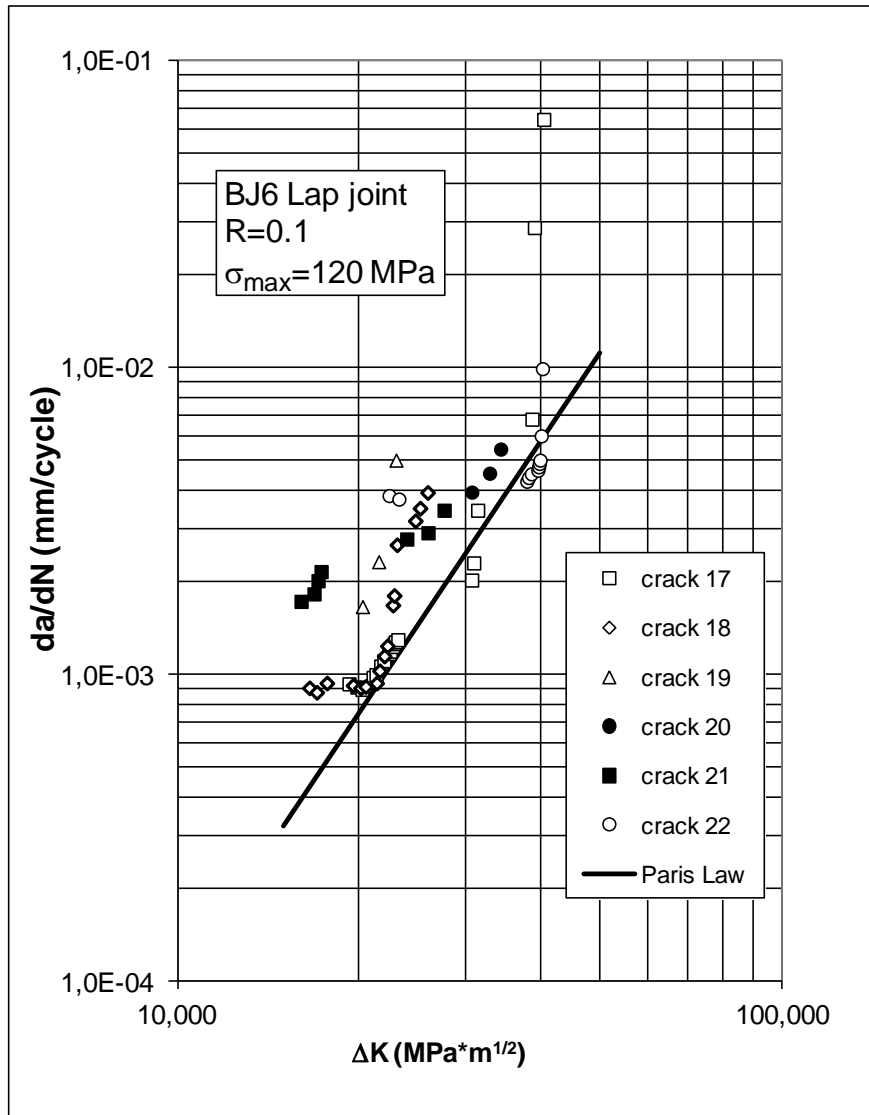


Fig. 9 Experimental crack growth rate and Paris law prediction (BJ6, $\gamma=0.85$)

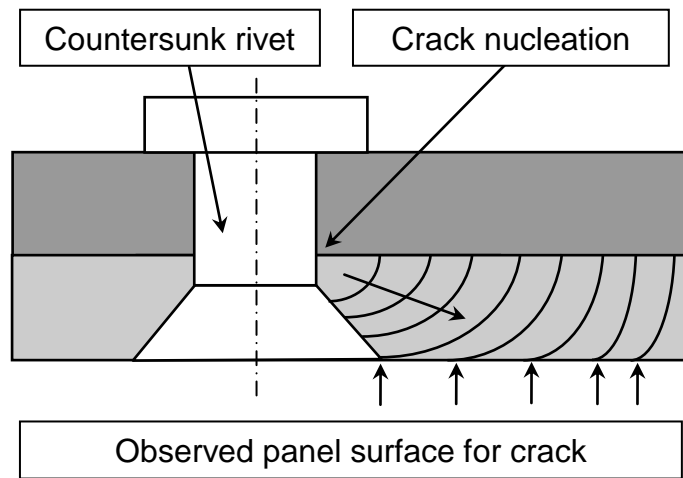


Fig. 10 Corner crack front evolution during crack propagation